SPECTRAL DECOMPOSITION AND AVO-BASED AMPLITUDE DECOMPOSITION: A COMPARATIVE STUDY AND APPLICATION

MOHAMMED FARFOUR[1], WANG JUNG YOON [2], SAID GACI [3] and NOUREDDINE OUABED [4]

[1] *Earth Science Dept., Sultan Qaboos University, Oman.*
[2] *Energy & Resources Engineering Dept., Chonnam University, Gwangju, South Korea.*
[3] *Algerian Institute of Petroleum, Boumerdes, Algeria.*
[4] *Sinopec Geophysical Corporation, Algiers, Algeria. wjyoon@chonnam.ac.kr*

(Received December 8, 2018; revised version accepted February 10, 2020)

ABSTRACT

Farfour, M., Yoon, W.J., Gaci, S. and Ouabed, N., 2020. Spectral decomposition and AVO-based Amplitude Decomposition: a comparative study and application. *Journal of Seismic Exploration*, 29: 261-273.

Seismic data are very rich in information about rocks and fluids saturating their pores. As a result of their unique mineralogical compositions and fluid properties that discriminate them from their surroundings, hydrocarbon-saturated formations have proved to have their own characteristic frequencies at which they preferentially show up in seismic data. This has provided considerable support to interpretations of spectral decomposition methods and led to great success in detecting hydrocarbons in many basins of the world. Early works in Amplitude Variation with Offset (AVO) proved that geological formations containing hydrocarbons have also their own amplitude expressions with which they respond to seismic excitations. These seismic responses are controlled by their lithology type, pore space, and fluid content. This in turn has supported interpretations of strong amplitude anomalies observed at top of hydrocarbon-saturated reservoirs and led to the success of AVO in many areas around the globe. In this study, AVO-based amplitude decomposition is introduced as a new way to look at seismic amplitudes from AVO. The amplitude decomposition is compared with the decomposition of frequencies concept and methods. Both decompositions are examined over a gas-saturated sandstone from Alberta, Canada. Results demonstrated that decomposing both amplitude and frequency of seismic data into their constituent components can help detect more reliable expressions from fluid-saturated formations. The study shows that the Intercept and Gradient can be used to reproduce partial stacks and also gathers and suggests that the two attributes can be thought of as alternative products to partial stacks.

KEY WORDS: Amplitude Variation with Offset, spectral decomposition, hydrocarbon.

0963-0651/20/$5.00

INTRODUCTION

Frequency of seismic traces are thought of as a superposition of different individual frequencies (Tai et al., 2009; Castagna et al., 2006). To retrieve these individual frequencies, a number of methods have been proposed and published in literature; this include but not limited to Short Time window Fourier Transform (STFT), Wavelet Transform (Chakraborty and Okaya, 1995; Sinha et al., 2005), S-Transform (ST) by Stockwell et al. (1996), Matching Pursuit Decomposition (MPD) by Liu and Marfurt (2007). Empirical Mode Decomposition methods represent a new generation of the spectral decomposition methods. The latter methods decompose seismic traces into intrinsic oscillatory components without the need to a priori basis functions (Han, and Baan, 2013). Each oscillatory component has its characteristic frequency.

Hydrocarbon-saturated formations have proved to have their own characteristic frequency at which they preferentially show up in seismic data. This is because of their unique mineralogical and fluid properties discriminating them from their surroundings. This has provided considerable support to interpretation of spectral decomposition methods and led to great success in detecting hydrocarbons in different regions of the world (Chen et al., 2008; Tai et al., 2009; Yoon and Farfour, 2012; Farfour et al., 2015).

Seismic amplitudes of traces in stack section are a sum of individual amplitudes recorded at different angles of incidence (Hendrickson, 1999). Variations of these constituent amplitudes are found to be good indications of lithology and fluid types (Ostrander, 1984, Rutherford and Williams, 1989). For this purposes, several equations and approximations have been suggested and utilized to assess the rate of change of amplitudes from offset to another and used it as a tool for lithology discrimination and hydrocarbons detection.

Early works in Amplitude Variation with Offset (AVO) proved that geological formations containing hydrocarbons have their own amplitude with which they respond to seismic excitation; these seismic responses are controlled by their lithology type, pore space, and fluid content. This in turn has helped interpreting strong amplitude anomalies observed at top of hydrocarbon-saturated reservoirs and led to the success of AVO in many basins around the globe (Loizou et al. 2008; Mosquera et al., 2013; Farfour et al., 2018).

An increasing number of published studies demonstrated the usefulness of incorporating spectral decomposition and AVO for formation characterization. For example, Loizou and Chen (2012) have used AVO supported with spectral decomposition to differentiate between hydrocarbon and water saturated formations from UK. Yoon and Farfour (2012) have used AVO and spectral decomposition to map a thin producing channel from Alberta, Canada.

In this work, we compare between spectral decomposition and AVO-based amplitude decomposition from different aspects. We then use both of decompositions to study the expressions of gas-producing formation from Alberta, Canada.

THEORIES AND METHODS

Frequency decomposition

The amplitude spectrum of seismic data can be decomposed into individual frequencies using several methods. We select wavelet based-decomposition as an example. A wavelet is defined as a function ψ(t) with a zero mean, localized in both time and frequency. By dilating and translating this wavelet ψ(t), we produce a family of daughter wavelets:

$$\psi_{\sigma,\tau}(t) = 1/\sqrt{\sigma}\,\psi((t-\tau)/\sigma) \quad , \tag{1}$$

where *σ, τ are real. σ* is the dilation parameter or scale (*σ ≠ 0), and τ is the translation parameter*. Note that the wavelet is normalized such that the L2-norm ||ψ|| is equal to unity.

The CWT is defined mathematically as the inner product of the family of wavelets $\psi_{\sigma,\tau}(!)$ with the signal *s*(*t)*.

$$S_{\omega}(\sigma,\tau) = \int_{-\infty}^{\infty} s(t)(\,1/\sqrt{\sigma})\bar{\psi}((t-\tau)/\sigma\,)dt \quad , \tag{2}$$

where $\bar{\psi}$ is the complex conjugate of ψ and S_{ω} is the time scale map (scalogram) (Sinha et al., 2005).

In this study we use the Mexican hat wavelet, one of the very commonly used wavelets in seismic spectral decomposition.

In practice, the CWT approach involves the following steps:

1. Decomposing the seismogram into wavelet components, as a function of the scale *σ* and the translation shift ***τ*.**
2. Multiplying the complex spectrum of each wavelet used in the basis function by its CWT coefficient and sum the result to generate instantaneous frequency gathers.
3. These gathers are then sorted to produce constant frequency cubes, time slices, or vertical sections (Chopra and Marfurt, 2007).

Although, they are different in the way they perform the decomposition of the spectra, all the decomposition methods aim to extract the constant frequency sections or cubes. Once these constant frequency sections are computed, the user can investigate and analyze the frequency expressions of

the targeted zone or formation. The latter expressions might be used to infer fluid presence, lithology changes, or thickness estimations (Farfour and Gaci, 2018).

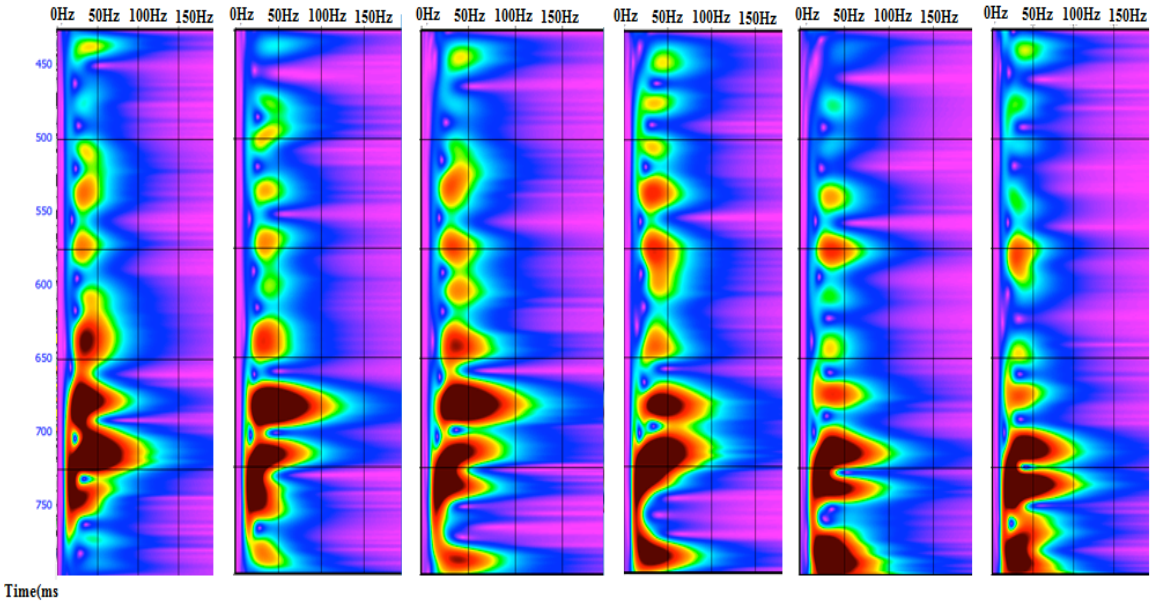

Fig. 1. Instantaneous frequency gathers extracted from seismic traces using CWT.

Amplitude decomposition

The Zoeppritz (1919) equations allow geophysicists to derive the exact plane-wave amplitudes of a reflected P-wave, as a function of angle. Over the years, a number of approximations to these equations have been published in literature (e.g., Aki and Richards, 1980; Wiggins et al., 1983; Shuey, 1985). The proposed form of Aki and Richards' (1980) approximation expresses the seismic amplitude in terms of changes in density, P-wave velocity, and S-wave velocity, across the interface between stratigraphic layers. The Aki-Richards approximation is widely accepted and used to compute AVO attributes, namely, the zero-offset reflections called intercept and the rate of change of the amplitude from angle to another called gradient. With these two attributes the amplitude can be formulated at different angles as

$$R(\theta) = R_p + G\sin^2\theta; \quad (3)$$

$R(\theta)$ is the reflection coefficient at angle theta, R_P is the intercept, while G is the gradient. This equation is applicable up to 30 degrees. By averaging amplitudes recorded at the different angles, the amplitude of stacked traces can be expressed as:

$$R_{stack} = \frac{1}{n}[R_p + R_p + G\sin^2(\theta_1) + R_p + G\sin^2(\theta_2) + \cdots + R_p G\sin^2(\theta_{n-1})] \quad . \quad (4)$$

The equations above suggest that if the intercept and gradient are known, the reflection coefficients contributing to the fully or partially stacked traces can be predicted and retrieved at any angle within the interval of the validity of the approximation. In other words, this makes it possible to inspect the seismic responses of geological formations at any angle of incidence. Accordingly, the intercept can be thought of as the amplitude component computed at zero angle. It is worth noting that there are other approximations that can be utilized for the same decomposition purpose. The interpreter can for example carry out the amplitude decomposition using Aki-Richards 3-term approximation, Shuey's 3-term approximation, or the exact solutions of Zoeppritz equations which are commonly invoked to compute amplitudes at larger angles with better accuracy than the two term-approximation used in the example illustrated in this study.

Fig. 2 shows example of group of seismic traces contributing to stacked traces in stack section (left) and the section from stacking (right). In case of presence of prestack gathers, the decomposition can be done by just sorting the traces and displaying them in a form of common offset/angle sections. In a similar way to spectral decomposition, one, then, can go through the different constant angle sections to study the expressions of the formation of interest. The latter amplitude expressions might lead to fluid presence detection, lithology change, or thickness variation.

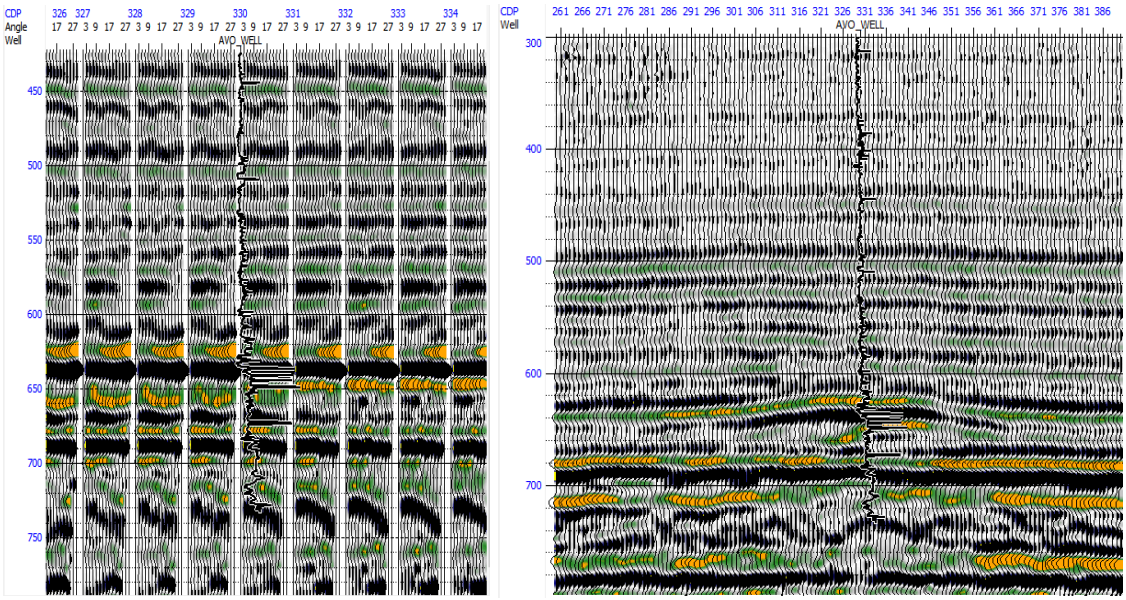

Fig. 2. Prestack gathers containing individual traces (left) composing the stack section (right).

Table 1 below summarizes the comparison between amplitude and spectral decomposition.

Table 1. Brief comparison between frequency decomposition and AVO based decomposition concepts and tools.

	Spectral decomposition	Amplitude decomposition
Objective	Decompose seismic data into individual frequency components	Computing amplitude individual component composing the stacked section
Tools	Numerous decomposition tools: for example CWT, STFT, MPD, ST, EMD (Huang et al. 1998), EEMD (Wu and Huang, 2009), CEEMD (Torres et al. 2011).	AVO approximations: Aki and Richards (1980) form; Wiggins et al. (1983) form; Shuey, 1985, or extracted directly from gathers
Input	Stacked seismic data	Prestack gathers or Intercept and Gradient
Products	Spectral images at constant frequencies	Amplitude images at constant angles

It is important to point out that the Zoeppritz equations and their approximations are derived for a single interface, separating two isotropic materials, assuming an incident plane wave. If one of the layers is anisotropic, then a modified form of the Zoeppritz equations must be used to compute the AVO attributes (Downton et al., 2000). In addition, when multiple interfaces and layers are present, factors that influence the amplitude such as multiples, converted waves, transmission losses all occur; thus, data must be appropriately processed in an AVO friendly fashion (Downton et al., 2000; Chopra and Marfurt, 2007). Therefore, for every play, the elastic parameters of the geologic objective must be understood and AVO modeling must be carried out before running AVO analysis on real data (Downton et al., 2000; Li et al., 2007)

We attempt herein to explore a real seismic data for indications about hydrocarbon responses. The target is gas-saturated sand located from Alberta Canada. We, first, use CWT to investigate its frequency behavior; after that, we deploy Aki-Richard equation to compute amplitude sections at different angles.

APPLICATION

We first commence our analysis with evaluating results from spectral decomposition. Figs. 3 and 4 depict frequency images at low frequency (10Hz), middle frequency (15 Hz) and higher frequency (25, and 40 Hz), respectively. It is readily seen that frequency responses are changing from frequency component to another. This can be related to the characteristic frequencies of the formations that are controlled by their physical properties

(lithology and thickness) and fluid content (Chen et al., 2008; Tai et al., 2009).

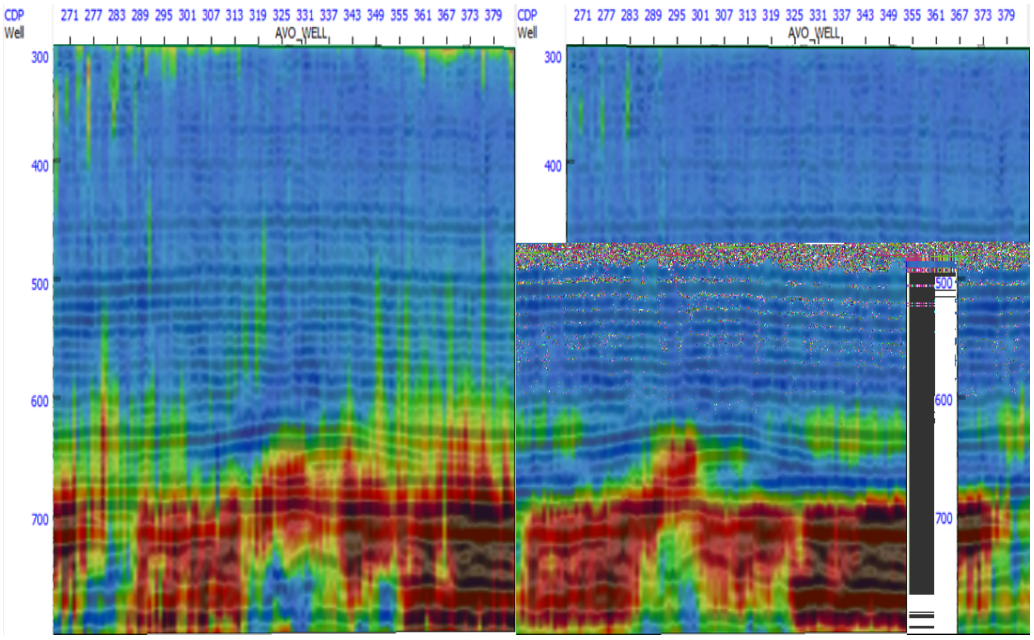

Fig. 3. 10-Hz and 15 Hz frequency images showing high amplitude at formations below reservoir.

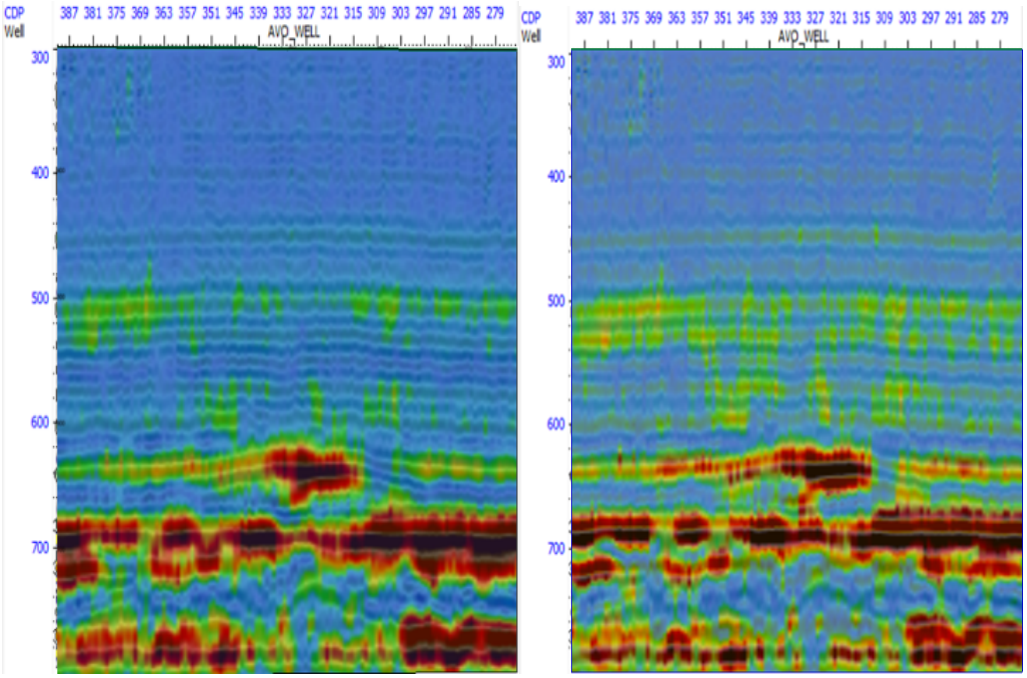

Fig. 4. 25-Hz and 40-Hz frequency images showing strong anomaly at the reservoir level.

It is noted also that the reservoir interval did not respond to the very low frequency. But at 10 Hz, an anomalous response shows up below the reservoir. This frequency response has disappeared at higher frequencies. Castagna et al. (2003) have observed this sort of low frequency anomalies in formations where the thickness is not sufficient for significant attenuation. At the high frequency component, the reservoir shows up clearly and a strong anomaly is observed at the central part of the top. This strong anomaly is interpreted to be caused partly by the presence of the hydrocarbons which are concentered at this part of the formation and also to the tuning effect which tends to magnify it.

Next, amplitude responses at different angles were computed using eq. (4) and displayed in Figs. 5 and 6. The near angle section shows responses of the different formations. At near offset, P-wave dominates the seismic responses and shows mostly the effect of changes in P-wave impedances between formations. At middle offset, the reservoir top response starts appearing different. The reservoir response becomes very clear and stands out as offset increases. The far angle section shows a strong anomaly that is not observed in surrounding formations.

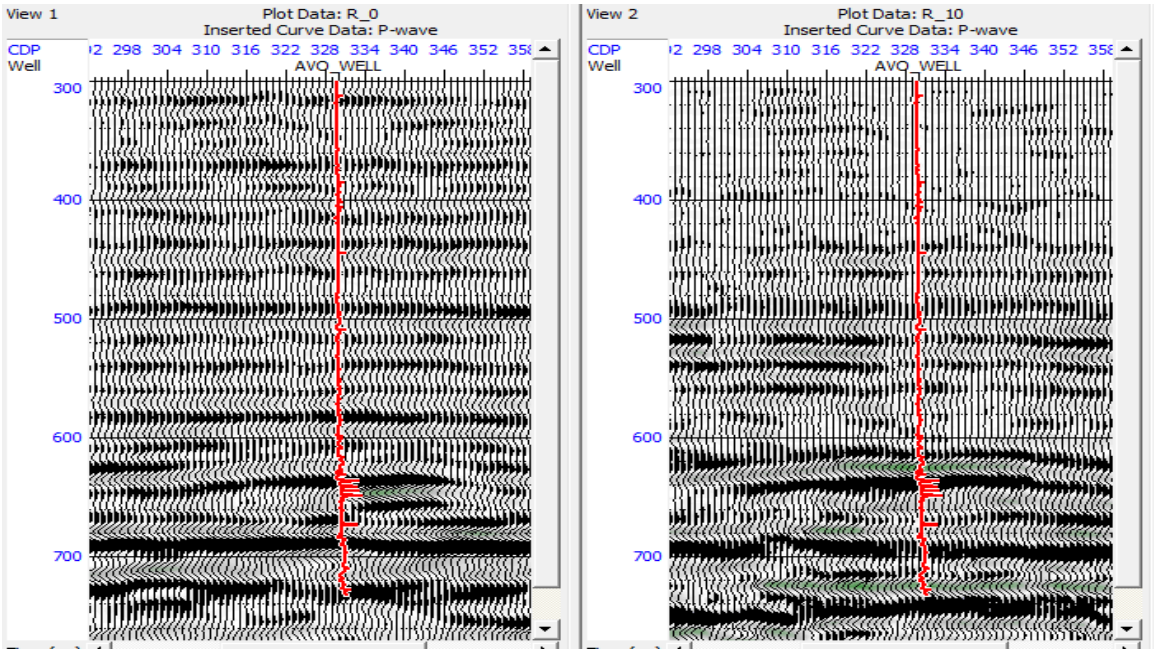

Fig. 5. Amplitude response at Zero-offset (left) and near-offset (right). Only slight change in amplitude is observed.

Constant angle sections were extracted from the gathers and displayed along with sections computed using AVO equation in Figs. 7 and 8. The sections exhibit almost similar behavior and distinguish the target formation from its surrounding. The advantage that can be noticed in the computed

sections over the section produced from the gathers is that the formers provide more complete information that are missing in the later. In fact, Figs. 9 and 10 show the zero-offset (or angle) sections and 29-degree angle sections from both decompositions. Note that the real gathers do not include zero-offset traces and only some intervals are available at the very far offset, but the computed sections did predict the missing information in both extreme angles.

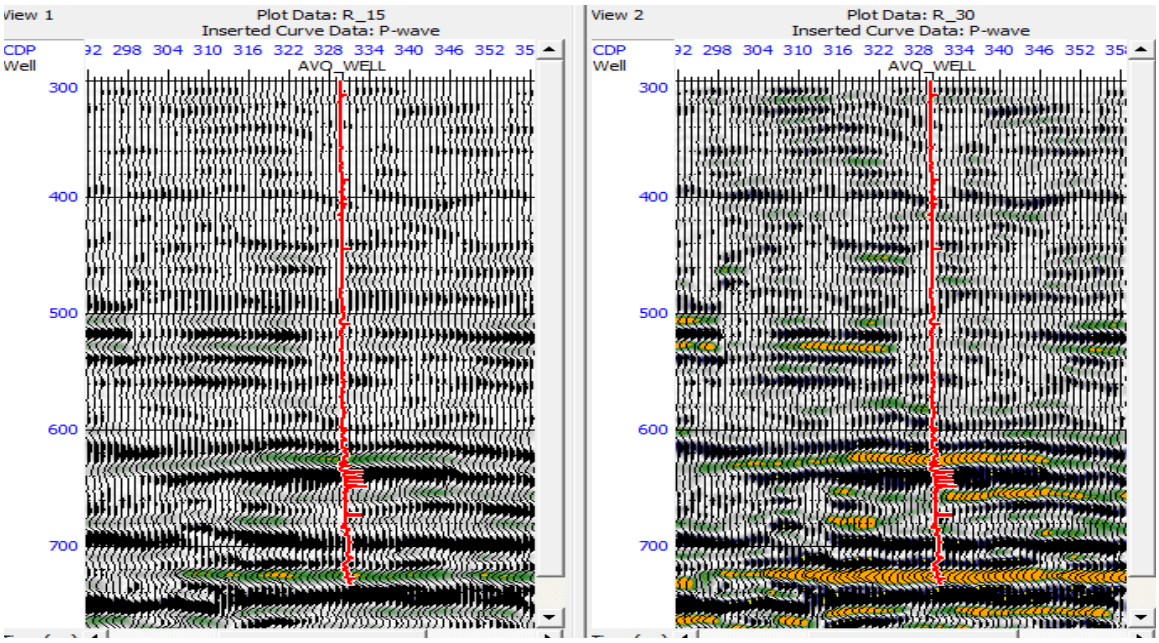

Fig. 6. Amplitude responses displayed at Middle (left) and far-offset (right). Remarkable changes are readily seen at reservoir level at 630 ms.

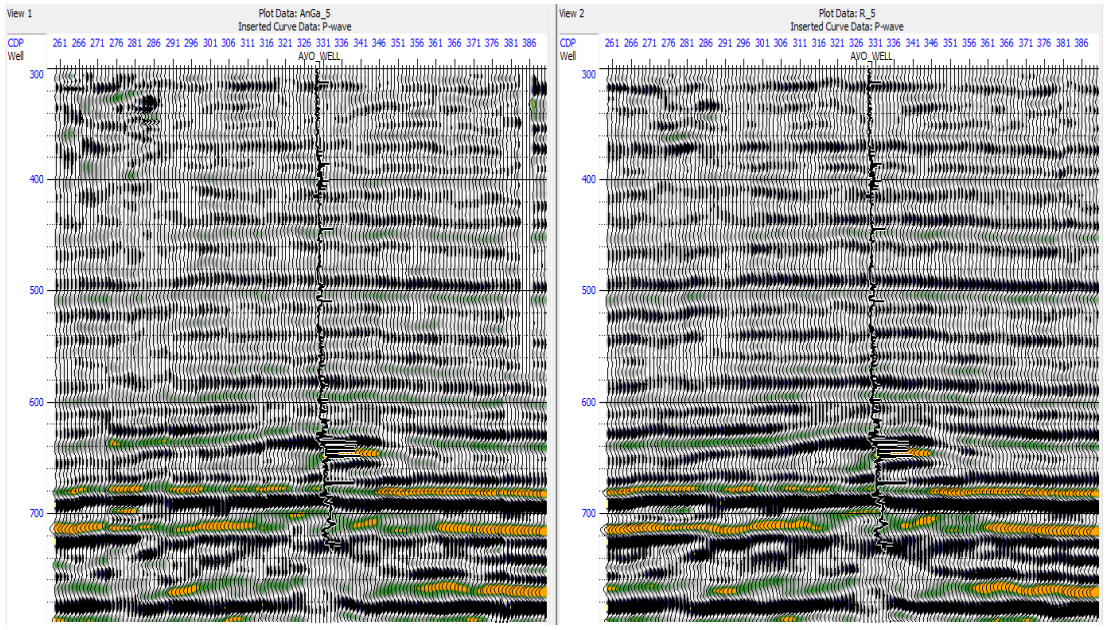

Fig. 7. Amplitude calculated at 5 degrees compared with the section derived directly from gathers.

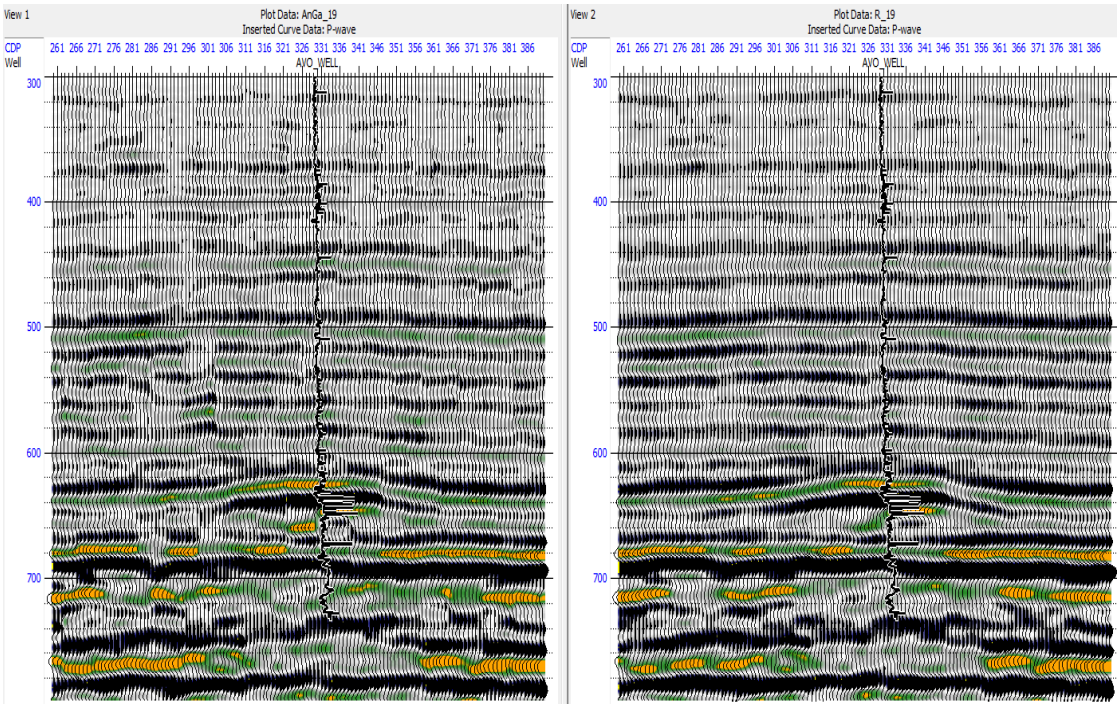

Fig. 8. Amplitude calculated at 19 degrees compared the section derived directly from gathers. The sections look very similar.

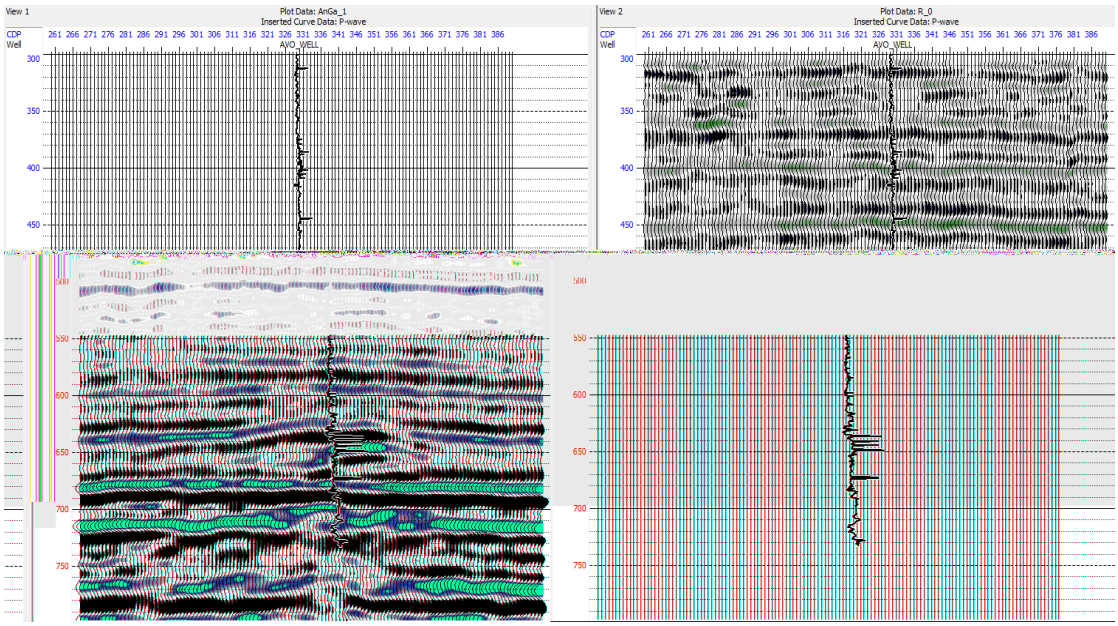

Fig. 9. Amplitude calculated at 0 degree (the right) compared with the section derived directly from gathers (left). Zero-offset traces are not present in the gathers but are available in the computed section.

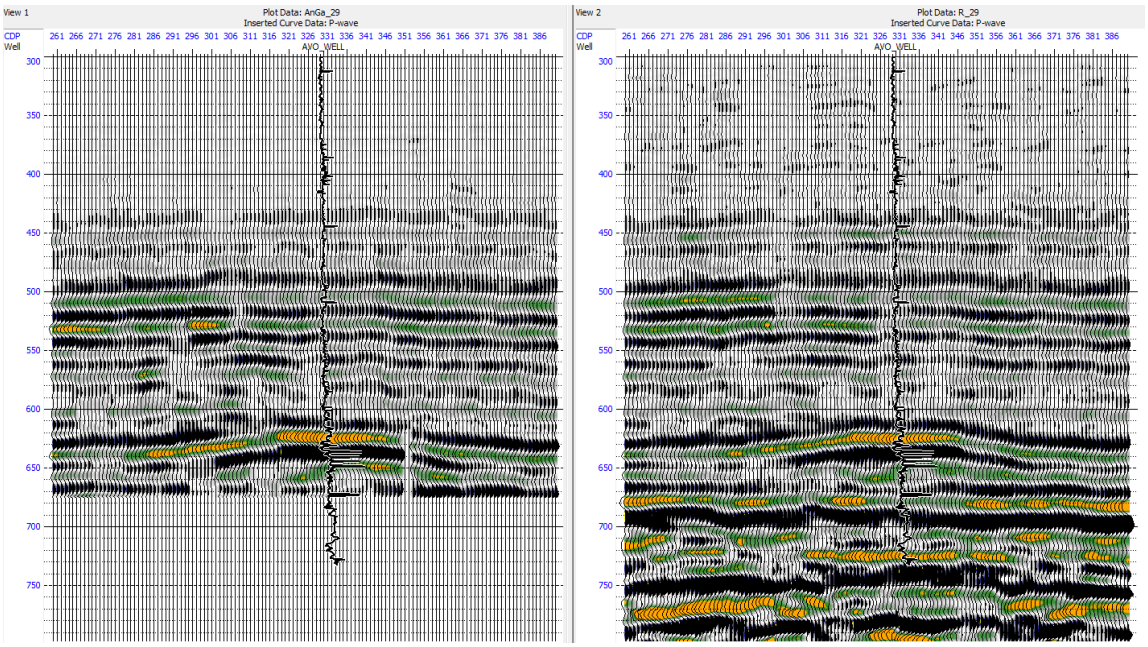

Fig. 10. Amplitude calculated at 29 degrees (right) compared the section derived directly from gathers (left). Notice that the lower part is missing in the produced section but is present in the computed section.

With the help of the equations above, we demonstrate that the intercept and gradient can also be used to reproduce partial stack sections and more importantly the prestack gathers. Fig. 11 displays gathers reproduced from the intercept and gradient compared with original gathers from processing.

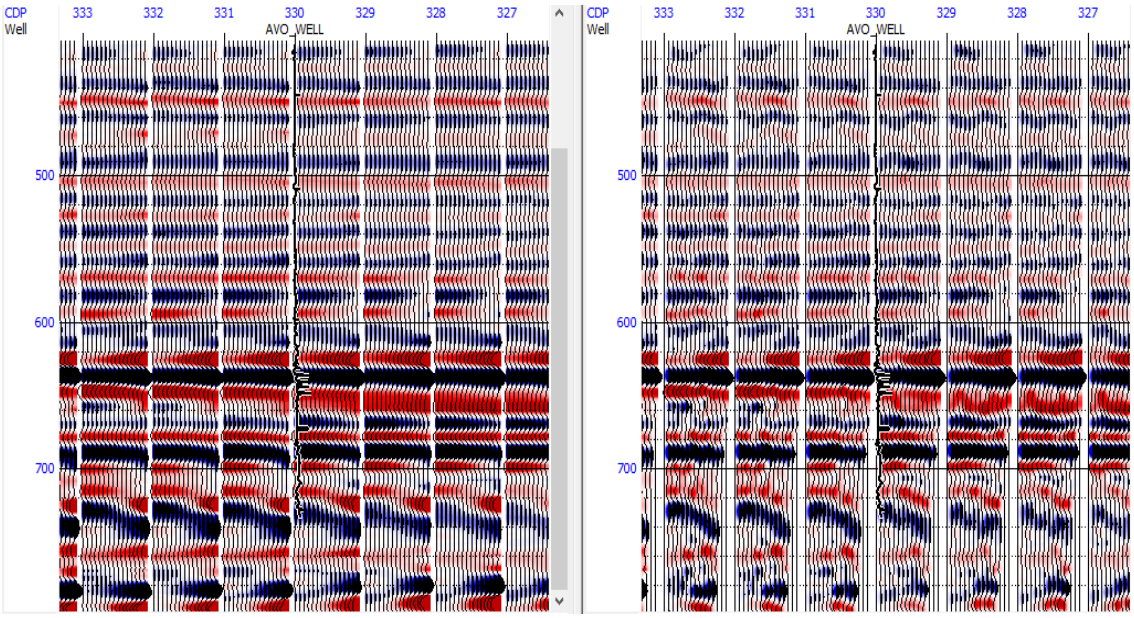

Fig. 11. Prestack gathers reproduced from intercept and gradient (left) and original gathers (right).

Although they look smoother, the calculated gathers exhibit very clear similarity to the real gathers. Thus, one can suggest including intercept and gradient cubes as deliverable products instead of partial stacks or providing them along with partial stacks. Note that intercept and gradient can also be obtained from partial stacks (see for example Mosquera et al., 2013). Once are determined, the two attributes can be used to compute the constant angle amplitude sections as described above.

CONCLUSION

A new look at amplitude variation with offset concept is presented. Approximations used for analyzing amplitude variation with offset are used to look at amplitude components in a way similar to frequency components derived from spectral decomposition. As an application, spectral decomposition and AVO-based amplitude decomposition have been used to differentiate geological formations based on their frequency and amplitude responses. The analysis of responses from both frequency and amplitude of geological formations showed that hydrocarbon-saturated targets can be recognized using amplitude and spectral decomposition methods. They exhibit responses that distinguish them from their surroundings.

The amplitude decomposition showed that if the intercept and gradient are properly prepared, they can help predict amplitude responses when very near or far offset gathers are not available or of poor quality, or in case only angle-stacks are accessible.

ACKNOWLEDGMENT

We would like to thank CGG's HampsonRussell for providing the software and data. Our thanks go also to dGB Earth Sciences for providing OpendTect software.

REFERENCES

Aki, K. and Richards, P.G., 1980. Quantitative Seismology: Theory and Methods. W.H. Freeman and Co., San Francisco, CA.

Castagna, J.P., Sun, S. and Siegfried, R.W., 2003. Instantaneous spectral analysis: Detection of low-frequency shadows associated with hydrocarbons. The Leading Edge, 22: 120-127.

Chakraborty, A. and Okaya, D., 1995. Frequency-time decomposition of seismic data using wavelet-based methods. Geophysics, 60: 1906-1910.

Chen, G., Matteucci, G., Fahmi, B. and Finn, Ch., 2008. Spectral-decomposition response to reservoir fluids from a deepwater West Africa reservoir. Geophysics 73, C2-C30.

Chopra, S. and Marfurt, K.J., 2007. Seismic Attributes for Prospect Identification and Reservoir Characterization. SEG, Tulsa, OK.

Downton, J.E., Russell, B.H. and Lines, L.R. 2000. AVO for managers: pitfalls and solutions. CREWES Research Report, 12.

Farfour, M., Yoon, W.J. and Jang, S., 2016. Energy-weighted Amplitude Variation with Offset: an AVO attribute for low impedance gas sands. J. Appl. Geophys., 123(6): 167-177

Farfour, M. and Gaci, S., 2018. Spectral decomposition and amplitude decomposition to detect hydrocarbons: comparison and application. RDPETRO 2018: Res. Develop. Petrol. Conf., Abu Dhabi, UAE, May 2018: 144-147.

Farfour, M., Yoon, W.J. and Kim, J. 2015. Seismic attributes and acoustic impedance inversion in interpretation of complex hydrocarbon reservoirs. J. Appl. Geophys., 111: 66-75.

Han, J. and van der Baan, M., 2013. Empirical mode decomposition for seismic time-frequency analysis. Geophysics, 78(2): O9-O19.

Hendrickson, J., 1999. Stacked. Geophys. Prosp., 47: 663-705.

Huang, N.E., Shen, Z., Long, S.R., Wu, M.C., Shih, H.H., Zheng, Q., Yen, N.-C., Tung, C.C. and Liu, H.H., 1998. The empirical mode decomposition and the Hilbert spectrum for nonlinear and non-stationary time series analysis. Proc. Roy. Soc. London, Series A: Mathemat., Phys. Engineer. Sci., 454: 903-995.

Li, Y., Downton, J. and Xu, Y., 2007. Practical aspects of AVO modeling. The Leading Edge,

Loizou, N. and Chen, S., 2012. The application and value of AVO and spectral decomposition for derisking Palaeogene prospects in the UK North Sea. First Break, 30: 55-67.

Ostrander, W.J., 1984. Plane-wave reflection coefficients for gas sands at non-normal angles of incidence. Geophysics, 49: 1637-1648.

Rutherford, S.R. and Williams, R.H., 1989. Amplitude-versus-offset variations in gas sands. Geophysics, 54: 680-688

Shuey, R.T., 1985. A simplification of the Zoeppritz equations. Geophysics, 50: 609-614.

Sinha, S., Routh, P., Anno, P. and Castagna, J.P., 2005. Spectral decomposition of seismic data with continuous-wavelet transform. Geophysics, 70(6): P19-P25.

Stockwell, R.G., Mansinha, L. and Lowe, R.P., 1996. Localization of the complex spectrum: the S transform. IEEE Transact. Signal Process., 44: 998-1001.

Tai, S., Puryear, P. and Castagna, J.P., 2009. Local frequency as a direct hydrocarbon indicator. Expanded Abstr., 79th Ann. Internat. SEG Mtg., Houston: 2160-2164.

Torres, M.E., Colominas, M.A., Schlotthauer, G. and Flandrin, P., 2011. A complete ensemble empirical mode decomposition with adaptive noise. IEEE Internat. Conf. Acoust., Speech Signal Process. (ICASSP): 41444147

Wiggins, R., Kenny, G.S. and McClure, C.D., 1983. A method for determining and displaying the shear-velocity refiectivities of a geologic formation. European Patent Applicat. 0113944.

Wu, Z. and Huang, N.E., 2009. Ensemble empirical mode decomposition: A noise-assisted data analysis method. Advan. Adapt. Data Analys., 1: 141.

Yoon, W.J. and Farfour, M., 2012. Spectral decomposition aids AVO analysis in reservoir characterization: a case study of Blackfoot field, AB, Canada. J. Computers Geosci., 46: 60-65.

Zoeppritz, K., 1919. Erdbebenwellen VIIIB, On the reflection and propagation of seismic waves. Göttinger Nachrichten, I, 66-84.